Article:

Carey, J.M., Cosgrove, B., Norton, K. et al. (3 more authors) (2021) Debris flow-slide initiation mechanisms in fill slopes, Wellington, New Zealand. Landslides, 18 (6). pp. 2061-2072. ISSN 1612-510X

https://doi.org/10.1007/s10346-021-01624-6

Laboratory simulations subaqueous mass movement generated by episodic undrained loading during earthquakes

Carey, J.M[1]., Mountjoy, J.J[2.]., Crutchley, G.J[3.,] , Petley, D.N.[4,] Holden, C[1]., Kaneko, Y[1,5].,
[1] GNS Science, 1 Fairway Drive Avalon, PO Box 30368 Lower Hutt, New Zealand
[2]National Institute of Water and Atmospheric Research, PO Box 14901, Wellington, New Zealand
[3] GEOMAR Helmholtz Centre for Ocean Research, Kiel, Germany
[3]Department of Geography, University of Sheffield, Sheffield, S10 2TN, UK
[3]Kyoto University Japan

ABSTRACT

Subaqueous slopes formed on active continental margins are subject to a variety failure styles, but their movement mechanisms during earthquakes remain poorly constrained as few submarine landslides have been directly sampled for detailed investigation. We conducted a series of dynamic shear experiments on samples recovered from the base of the Tuaheni Landslide Complex, located off the east coast of the North Island of New Zealand, to explore its potential behaviour during earthquakes. Our experiments suggest that while liquefaction could occur in marginally stable subaqueous slopes, particularly in shallow sediments on steep slopes or sediments with high initial pore fluid pressures, this is not a likely failure mechanism for pre-existing deep landslide complexes such as the Tuaheni Landslide Complex. Subaqueous landslides occurring along deeper, shallow angled shear zones are likely to experience episodic displacement when pore water pressures are sufficiently elevated during large earthquakes. The observed behaviour provides a credible mechanism through which subaqueous landslides in similar materials and active tectonic settings may be subject to episodic movement without undergoing catastrophic failure.

1. INTRODUCTION

Recent advances in submarine slope surveys (e.g. ref), sub-surface investigation (e.g. Barnes et al. 1991), and modelling (e.g. Urlaub et al. 2015) have allowed submarine mass movement process to be studied with unprecedented accuracy. These studies have revealed that many subaqueous mass movements initiate on shallow slopes (<2°) with gradients significantly lower their constituent materials (e.g. Barnes et al. 1991; Urlaub et al. 2015). Despite this many subaqueous slope failures runout over long distances (Tailing et al., 2007) and evacuate almost all the material from their source regions (Krastel et al., 2018; Mountjoy and Micallef, 2018). To explain this, conventional models frequently propose the presence of high pore fluid pressures that greatly exceed hydrostatic pressure. These models have been supported by laboratory and modelling studies that indicate high pore fluid pressures could be generated through undrained cyclic loading during earthquakes (e.g. Sassa et al. 2012), the generation of excess pore water pressures during sediment burial (e.g. Stigall and Dugan 2010), concentrated fluid flow (e.g. Dugan and Flemings, 2000; Sassa et al. 2012) or gas liberation from hydrate dissociation (e.g. Riboulot et al., 2013).

The landslide morphology of some subaqueous mass movements, however, indicate they have displaced over much shorter distances before arresting, even when their continued downslope movement is unconstrained (Locat and Lee, 2000; Micallef et al., 2013). These arrested landslide complexes can often be observed in close proximity to long run-out landslides in a wide range of seafloor environments including active margins that regularly experience seismic activity (Micallef et al., 2016). To date, however, the potential reactivation mechanisms and movement styles remain poorly constrained.

Terrestrial landslides also display a wide array of movement styles during earthquakes. Many recent terrestrial landslide inventories (e.g. Li et al., 2014; Valagussa et al., 2016; Massey et al., 2018) demonstrate that most of large catastrophic landslides occur adjacent to slopes with topographic characteristics show limited downslope movement despite being subject to similar ground shaking intensities (e.g. Collins and Jibson, 2015; Petley et al., 2006). Recent studies that accurately replicate dynamic loading scenarios in terrestrial landslide complexes during earthquakes have successfully shown how the shear surface deformations mechanisms control their movement patterns (e.g. Carey et al. 2019). Similar approach would be beneficial for submarine landslide complexes such studies have been rarely attempted because very few are accessible for sampling and detailed investigation.

The Tuaheni Landslide Complex (TLC), is located in an active subduction zone experiencing regular seismic activity and has a similar morphology to some slow-moving terrestrial landslides that often remobilise episodically without catastrophic failure. The (TLC) has been investigated by both shallow coring and seafloor drilling (Kuhlmann et al., 2018; Carey et al., 2019; Pecher et al. 2019) and is composed of subaqueous sediments common across the continental slope. Although the TLC is known to experience regular seismic activity (Wallace and Bevan, 2010; Wallace et al., 2012) its potential movement response to earthquakes has received limited attention to date as alternative drivers for slope destabilisation have been the focus of investigations (e.g. Mountjoy et al. 2014; Micallef et al. 2016).

In this study we have sought to understand better the potential movement mechanisms of a large submarine complex, using samples recovered from the site. We have conducted laboratory experiments in a dynamic back-pressured shearbox on sediments recovered from the base of Tuaheni Landslide Complex on the Hikurangi Subduction Margin, off the coast of Gisborne, New Zealand, to explore styles of movement under conditions that accurately replicate seismic loading in order to provide insight into the response of these materials, under representative stress states, to dynamic changes in stress state.

2. STUDY AREA

2.1. Landslide geomorphology

An area of the upper continental slope on the Hikurangi Subduction Margin hosts a number of landslides (Mountjoy et al., 2009; Micallef et al., 2016). The Tuaheni Landslide Complex (TLC) comprises an area of approximately 145 km2, which is sub-divided into two distinct elements (Tuaheni North and Tuaheni South) separated by a 2 km wide spur (Figure 1A). While Tuaheni North is formed of multiple evacuated landslide scarps, Tuaheni South is characterised by a large debris apron that has a distinct scarp and bench topography, and features indicative of lateral, extensional and compressional deformation (Mountjoy et al., 2009; 2014). The morphology of Tuaheni South is similar to slow-moving landslide complexes observed in terrestrial environments, such as earthflows and mudslides (e.g. Hungr et al., 2014), which occur in similar fine-grained sediments and are often subject to episodic remobilisation (e.g. Allison and Brunsden, 1990).

The upper continental slope is composed of Miocene to Recent slope basin sequences (Mountjoy et al., 2009). A gravity core profile along the length of the Tuaheni Landslide Complex has indicated that the upper few meters of sediment are dominated by mud to sand sized particles from hemipelagic drape, reworked landslide debris and airfall tephra (Kuhlmann et al., 2018). More recently sediments from the base of the TLC have been recovered from boreholes drilled in 2016 during the Mebo expedition (Fig 1 GeoB20802, Geo20831) and during the 2IODP expedition 372 in 2017 (Fig 1, U1517). These boreholes demonstrate that the base of the landslide (approx. 40 m bsf) is dominated by fine-grained sandy sediments with grain size characteristics that suggest they might be susceptible to liquefaction. The base of the landslide was found to be XX m above the base of gas hydrate stability (Fig. 1b)ty indicating that the development of overpressure from free gas is unlikely. As a consequence, the potential development of overpressure during seismic loading from earthquakes was considered a credible movement mechanism that warranted further exploration.

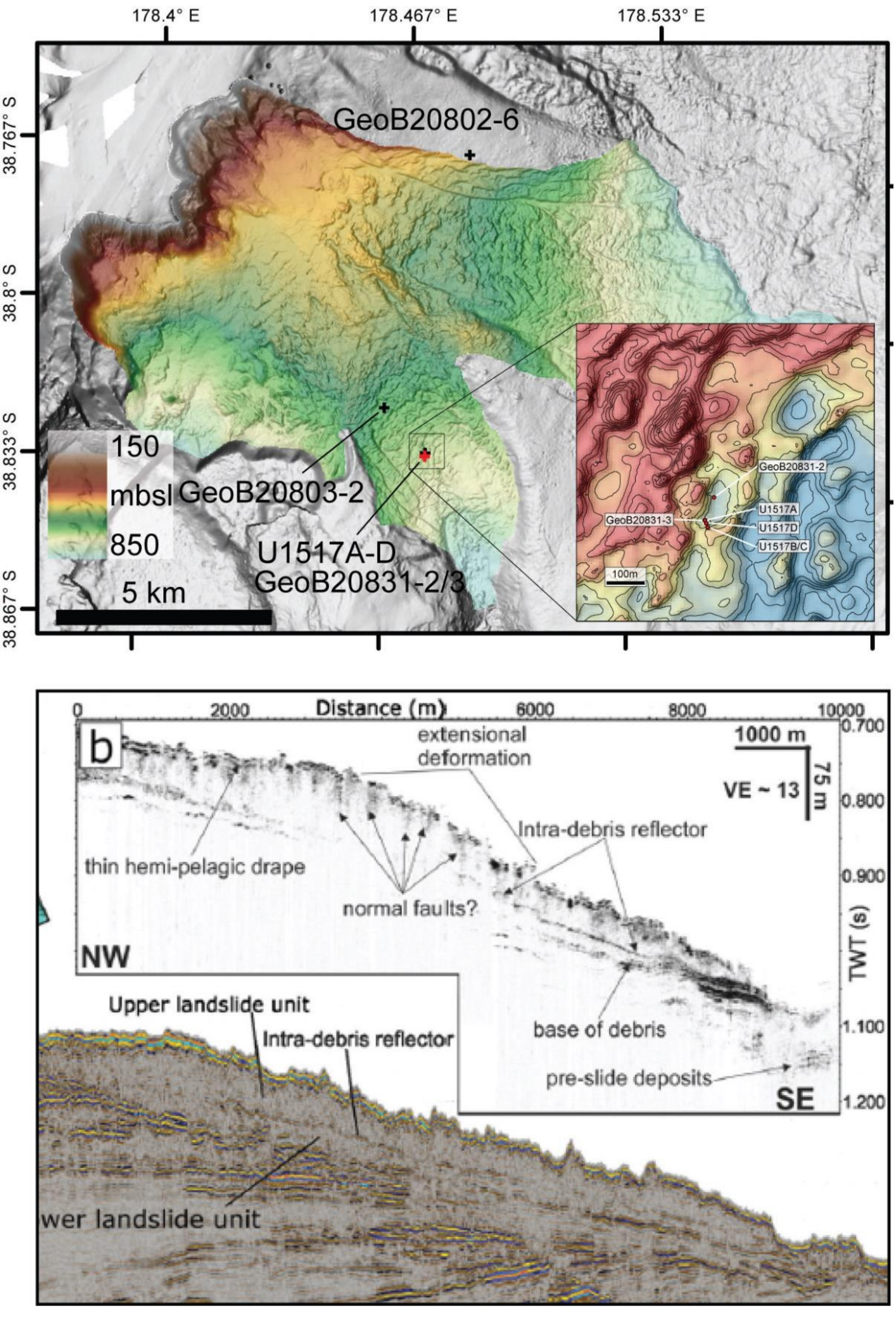

Figure 1. Site location Joshu modifying the above for paper

2.2 Regional seismicity and earthquake history

The landslide lies within an active subduction zone experiencing regular seismic activity (Wallace and Bevan, 2010; Wallace et al., 2012). The regional seismic hazard is characterized by earthquake activity on the Hikurangi subduction zone interface, on shallow crustal faults (such as the 1931 Napier earthquake) and on intraslab faults such as the 2007 M6.7 Gisborne event (GEq). In addition Tuaheni Basin is prone to moderate but long shaking from distant events such as the M7.8 Kaikōura (KEq) and M7.4 Te Araroa (TAEq) earthquakes (Kaneko et al DATE). Ground shaking at these regional sites can be subjected to strong amplification in the 0.5-5Hz frequency range due to shallow soft sediments (Perrin et al. ref) and strong amplification at periods of about 20 seconds from the deep offshore sediment basin (ref). The latter, however, are unlikely to influence ground motion triggering of the Tuaheni Landslide Complex which has a natural period between 0.5 and 5Hz.

Relatively small (cm-scale) displacements triggered in a large landslide complexes such as Tuaheni are likely generate a local tsunami that would be recorded on the nearby Gisborne tide gauge. This implies that ground shaking that does not trigger a local tsunami provides a lower band ground shaking threshold for landslide triggering. As neither of GEq, TAEq and KEq triggered local tsunamis, estimated peak ground shaking values near the landslide site for these events will define a lower band shaking threshold for landslide triggering. We employed two approaches to get peak shaking values. For the distant earthquakes TAEq and KEq, peak shaking at the landslide site will be similar to peak shaking 30 km away (reference) at GKBS (GeoNet network). For the regional earthquake GEq, local source effects will influence ground shaking even at close distances. Therefore, it is more appropriate to calculate synthetic ground shaking at the site.

In this study we convert shaking parameters into “stressgrams”. Dynamic stress at locations of interest, or “stressgrams” are better input parameters to model the various landslide responses and were derived using the following equation:

EQUATION

Three-component velocity seismograms were obtained for earthquakes TAEq and KEq at station GKBS. This station is located on site-class B type soil condition, equivalent to strong rock condition with little site amplification. The velocity seismograms are bandpass filtered between 0.5 and 5 Hz. The final stressgrams are shown in fig. xx.

Stressgrams for 2007 Gisborne earthquake:

The EXSIM code is finite fault stochastic modelling code that takes into account source as well as regional parameters (Motazedian and Atkinson, 2005) and was used to model the synthetic seismograms. The stochastic approach requires a well-defined source model, attenuation model, and quantification of site effects. These parameters are detailed in Holden (2020 - in prep) as well as the validation method. Even though the stochastic method does not model realistic phases of seismograms it was able to capture periods as long as 2 sec very well. Synthetic horizontal accelerations were integrated into velocity then bandpass filtered between 0.5 and 5Hz (Fig. 2).

Section on subduction zone earthquake

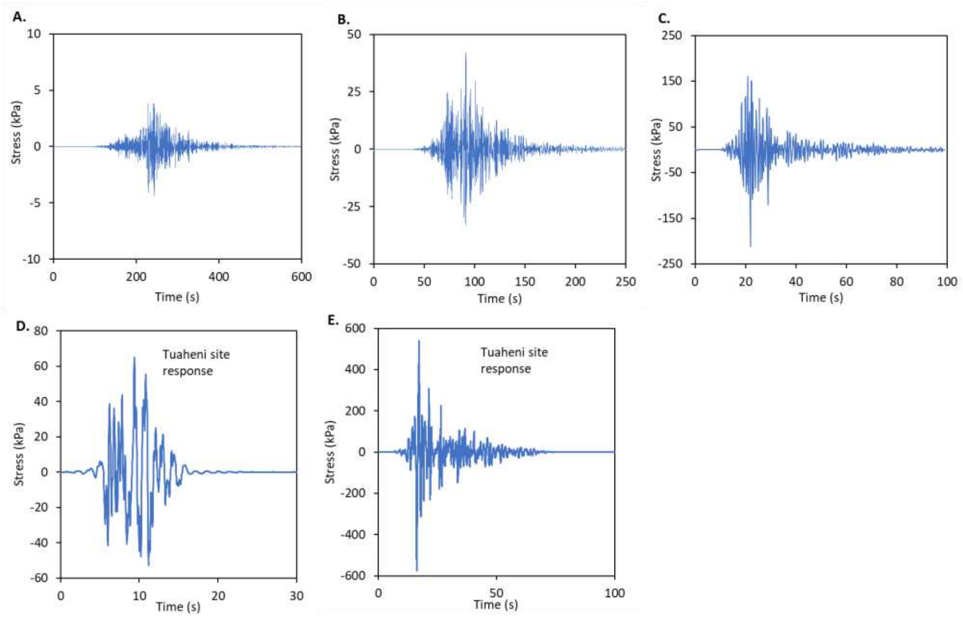

Figure 2. Stress changes during significant earthquakes, calculated from Seismogram data recorded in Gisborne (filtered between 0.5 and 5 Hz). (A) M7.8 Kaikoura Earthquake, measured at the Gisborne station (GKBS), 2016. (B) M7.1. Te Araroa earthquake, measured at Gisborne station (GISS), 2016. (C) M6.7 Gisborne earthquake, measured at Gisborne station (GISS), 2007. (D) Modelled local site response during the Gisborne earthquake. (E) Modelled site response during a Magnitude 8 subduction earthquake.

3. MATERIALS AND EXPERIMENT APPROACH

A suite of conventional laboratory experiments on TLC sediment samples collected from the boreholes Geo20831 during the Sonner Expedition SO247 in 2016 and U1517 during the IODP expedition 372 in 2017 (Fig 1) to determine their physical and geomechanical characteristics (Table 1).

These soil classification test results indicate that whilst natural moisture contents were broadly consistent (23% to 27%) across all samples, the landslide is composed sediment types (Table 1). Samples EN1403 EN1404, and EN1408 had soil classifications at the boundary of low plasticity silts and clays, characterized by lower bulk and dry densities, higher liquid limits and plasticity indexes (Table 1). In contrast samples EN1407, EN1409, EN1410 and EN1410 had soil classifications of fine sands, characterized by high bulk and dry densities, lower liquid limits and plasticity indexes (Table 1). Particle-size analyses confirmed two distinct grain size distributions (Figure 2). Coarse silt and fine sands accounted for over 80% of the material in the coarse-grained sediments whilst silts and clays accounted for over 80% of the material in the fine-grained sediments.

TABLE 1. PHYSICAL PROPERTIES OF TLC SEDIMENTS RECOVERED FROM BOREHOLES GEOBORE 30821 AND IODP U1518

Sample Reference	EN1403	EN1404	EN1405**	EN1406**	EN1407	EN1408	EN1409	EN1410	EN1411
Borehole	U1517	U1517	U1517	U1517	U1517	U1517	30821	30821	30821
Sample depth (*mbsb)	21.44 – 21.53	61.26 – 61.38	59.20 – 59.30	30.06 – 30.22	31.61 – 31.77	40.69 - 40.80	28.40 – 29.60	31.90 – 33.27	35.40 - 36.92
Moisture content (%)	27.2	23.0	-	-	24.6	26.9	23.3	23.3	24.3
Bulk density (kg/m³)	1.82	1.83	-	-	1.89	1.89	1.99	2.03	1.85
Dry density (t/m³)	1.43	1.49	-	-	1.54	1.49	-	-	1.48
Atterberg limits:									
Plastic limit (%)	28.0	20.0	-	-	25.2	22.1	23.1	26.4	23.1
Liquid limit (%)	48.1	38.5	-	-	33.2	43.4	34.2	31.8	34.3
Plasticity index (%)	20.3	18.5	-	-	8.0	21.3	11.2	5.4	11.2

*mbsb = meters below sea bed ** Samples not used for index testing

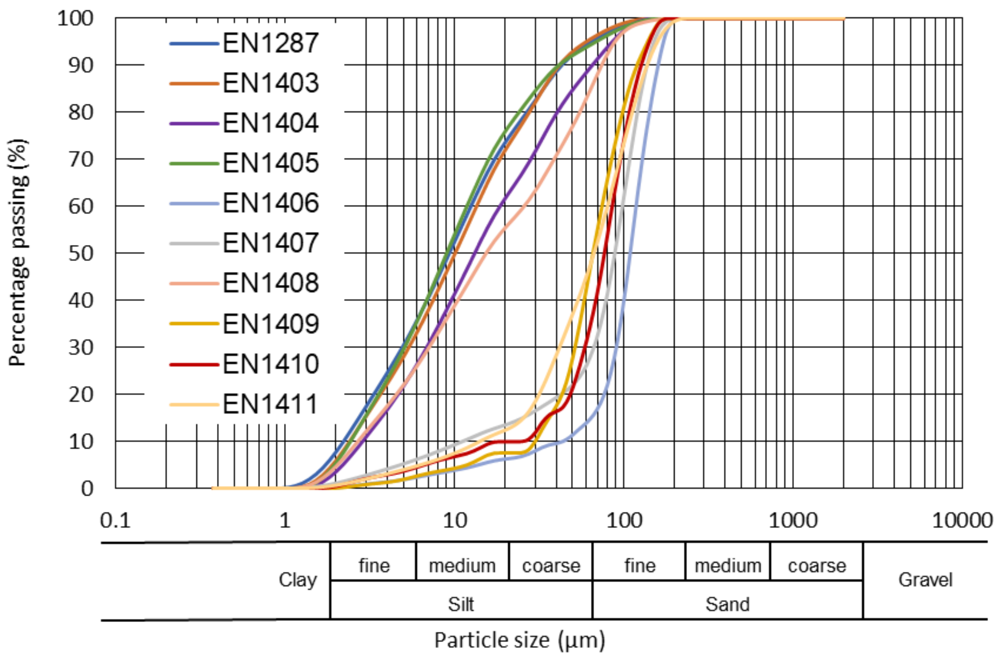

Figure 3. Particle size analysis of samples recovered from within the Tuaheni Landslide Complex (remove sample 1287 from figure).

Conventional monotonic drained direct shear tests were undertaken on 60 x 60 x 20 mm samples using a Wykeham Farrance direct shearbox WF2500. Shearing was conducted at three normal stresses (Table 2) and shearing was initiated on completion of the consolidation phase. A low shear rate (0.0018 mm/min), was used to avoid developing excess pore fluid pressures within the specimens.

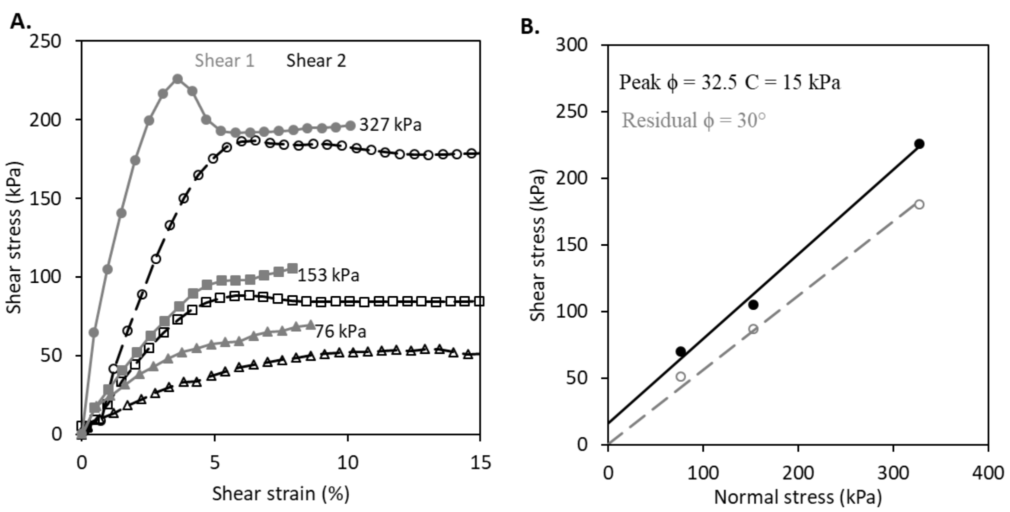

Figure 4. Conventional monotonic drained shear experiments. (A) Stress-strain behaviour. (B) Monotonic drained peak and residual strength envelopes.

The geomechanical properties derived from these conventional laboratory experiments were used to design a suite of dynamic shear experiments to simulate the effects of seismic loading at the base of the TLC. These experiments were undertaken in a Dynamic Back Pressured Shear Box (DBPSB), an advanced direct shear device that allows the measurement and control of pore pressures and dynamic application of normal stress and shear stress, which has been successfully used to explore a range of styles of deformation in landslide materials (e.g. Brain et al. 2015; Carey et al., 2016, 2019).

TABLE 2. SUMMARY OF THE DYNAMIC SHEAR EXPERIMENTS

Sample Number	Initial normal effective stress (kPa)	Initial shear stress (kPa)	Applied dynamic shear amplitude (+/-)	Applied normal stress	Dynamic frequency (Hz)	Number of Cycles
EN1410A	150	42	0.5 mm	150 kPa	0.5	30
EN1410B	150	64	0.5 mm	Volume controlled	0.5	30
EN1410C	-	10	25 kPa	Volume controlled	0.5, 2, 5	10
EN1410D	-	10	10,25,50 60 kPa	Volume controlled	0.5	30

4. LIQUEFACTION POTENTIAL DURING DYNAMIC SHEAR

To evaluate whether seismic loading could induce liquefaction in the fine-grained sediments at the base of the TLC we conducted strain controlled dynamic shear experiments on two fine-grained sand samples reconstituted from sample EN1410 (Table 2). Both samples were initially consolidated at a normal effective stress of 150 kPa to replicate burial depth of the basal materials in the landslide before an initial static shear stress of 65 kPa (approximately 70% of the conventional drained failure envelope) was applied to each sample to represent the stress state in a marginally stable landslide shear zone.

During the first experiment (EN1410A) the methodology described by Carey et al., 2016 was adopted in which the normal stress and back pressure were held constant while a displacement controlled dynamic shear phase was carried out whilst the development of excess pore water pressure and shear stress were measured. (Table 2). Dynamic shear resulted in a decrease in sample pore water pressures, which increased normal effective stress (Fig 6 A). Consequently, continued displacement required a progressive increase in shear stress throughout the experiment (Fig 6 A). The experiment did not generate undrained conditions in the sample, which instead followed a drained stress path and resulted sample densification and subsequent strain hardening (Fig 6 B).

To simulate the materials undrained behaviour during seismic loading, a testing procedure was adapted from a well-established dynamic simple shear methodology (Dyvik et al. 1987). Using this approach, a constant volume is maintained during dynamic shear and the measured change in applied normal stress as the specimen height is maintained is equal to the porewater pressure that would be generated in a purely undrained experiment (Dyvik et al. 1987). To replicate this a further experiment was conducted on sample EN1410B. (Table 2). In this experiment a constant sample volume was applied during dynamic shear by maintaining a constant sample height (axial displacement) and pore fluid volume (back volume) such that the reduction in mean effective stress resulting from the reduction in applied normal stress was equal to the excess porewater pressure anticipated in undrained conditions.

During the volume-controlled experiment dynamic shear resulted in a rapid reduction in mean effective stress over the first 10 cycles of loading, indicating the development of significant excess pore water pressures (Fig 6 C). This reduction in normal effective stress corresponded with a rapid loss in shear strength until no significant frictional strength could be measured (Fig 6 C). The stress path indicates that the failure envelope was reached during the first dynamic cycle and during further cycles the stress path followed the failure envelope as the sample underwent liquefaction (Fig 6 D). Thus, the fine sand forming the basal material of the TLC can undergo liquefaction as a result of seismic loading when subject to certain stress conditions. The volume-controlled experiments were able to replicate the undrained behaviour expected in landslide shear zone during seismic loading. Consequently this testing approach was adopted to further explore the potential movement behaviour of the TLC during earthquakes of varying magnitude and duration.

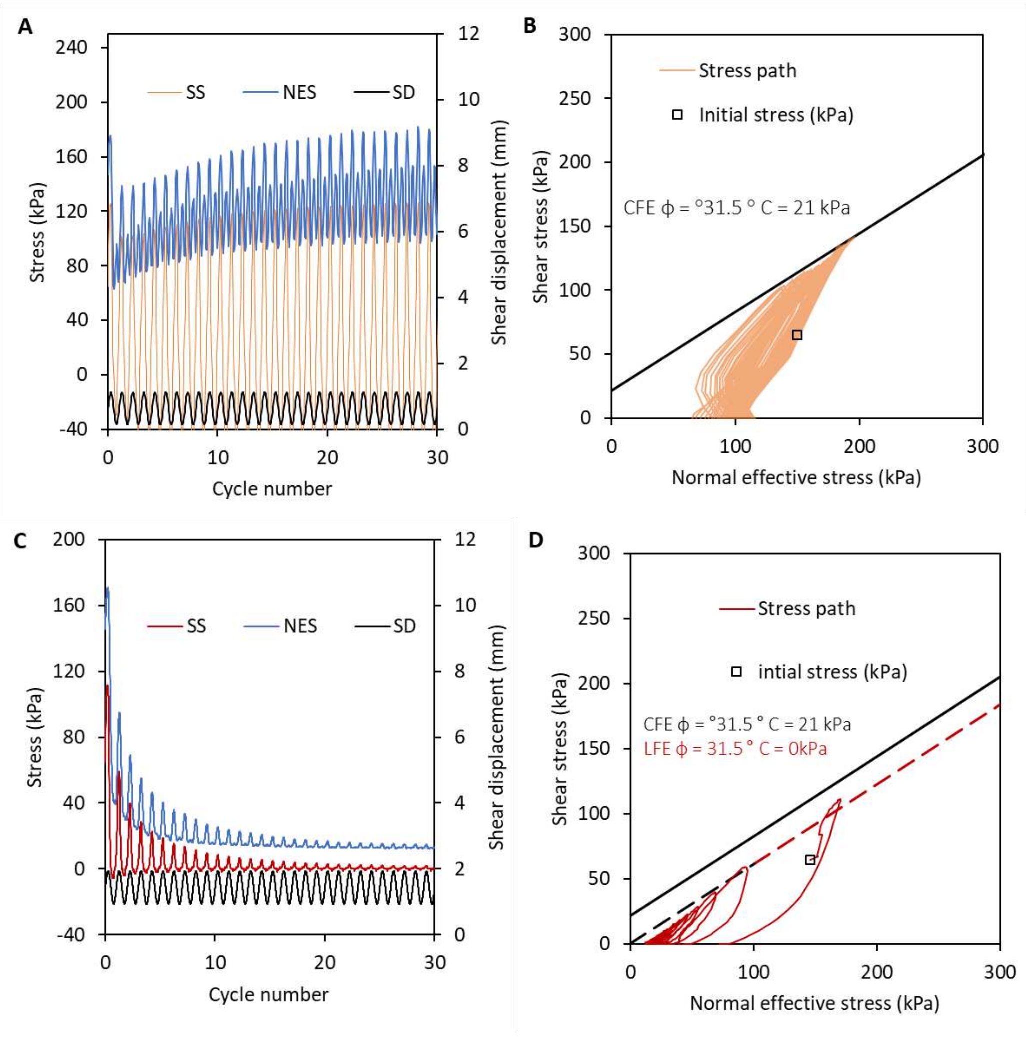

Figure 6. Strain controlled dynamic shear experiments (+/- 0.5 mm) conducted at a frequency of 2 Hz (A) Shear stress (SS) Normal effective stress (NES) and Shear displacement (SD) against cycle number during normal stress controlled dynamic shear experiment, Sample EN1410A (B) Stress path in relation monotonic failure envelope, sample EN1410A (C) Shear stress (SS) Normal effective stress (NES) and Shear displacement (SD) against cycle number during normal stress controlled dynamic shear experiment, Sample EN1410B (D) Stress path in relation monotonic failure envelope, sample EN1410B.

5. SIMULATING UNDRAINED BEHAVIOUR DURING DYNAMIC SHEAR IN THE TLC

To simulate undrained conditions within the basal shear zone of the TLC an initial normal effective stress was applied to samples EN1410C and EN1410D to generate consolidation. Thereupon, an initial shear stress of 10 kPa was applied to each sample (Table 2). This initial stress state, which is lower than in the previous experiments, was adopted to simulate the shear stress associated with the angle shear surface (c.2°) identified in geophysical interpretations of the landslide geometry (Crutchley et al. DATE). The initial pore water pressure was set to simulate hydrostatic conditions.

To explore the displacement behaviour of the TLC when subject to different frequencies of short duration, dynamic loading, sample EN1410C was subject to three separate dynamic stress-controlled shear stages (Table 2). In each case dynamic shear stress was applied over 10 cycles at progressively higher frequencies (Table 2). The initial normal effective stress and shear stress was reapplied to the sample between each dynamic shear stage (Fig 7 A, Table 2). During the first low frequency dynamic shear stage (0.5. Hz) dynamic loading resulted in progressively larger shear displacements, although the total cumulative displacement was comparatively small (Fig 7 B). These progressively increasing shear displacement cycles developed as the normal effective stress reduced (Fig 7 C) and indicated that the sample was strain softening during dynamic loading prior to reaching the conventional failure envelope (Fig 7 D). Less displacement was then observed during the second dynamic shear stage (2 Hz) despite a similar reduction in normal effective stress during dynamic loading. Similar behaviour was also observed during the third dynamic shear stage (5 Hz) as was accompanied by a much lower reduction in mean effective stress during dynamic loading, suggesting that the sample progressively strengthened between each dynamic stage as the initial normal stress was reapplied and pore fluids drained from the sample.

The results indicate that whilst short duration dynamic shear experiments could induce strain and excess porewater development, the reduction in normal effective stress was not sufficient to reach the conventional failure envelope and generate either significant permanent displacement or liquefaction (Fig 7 D).

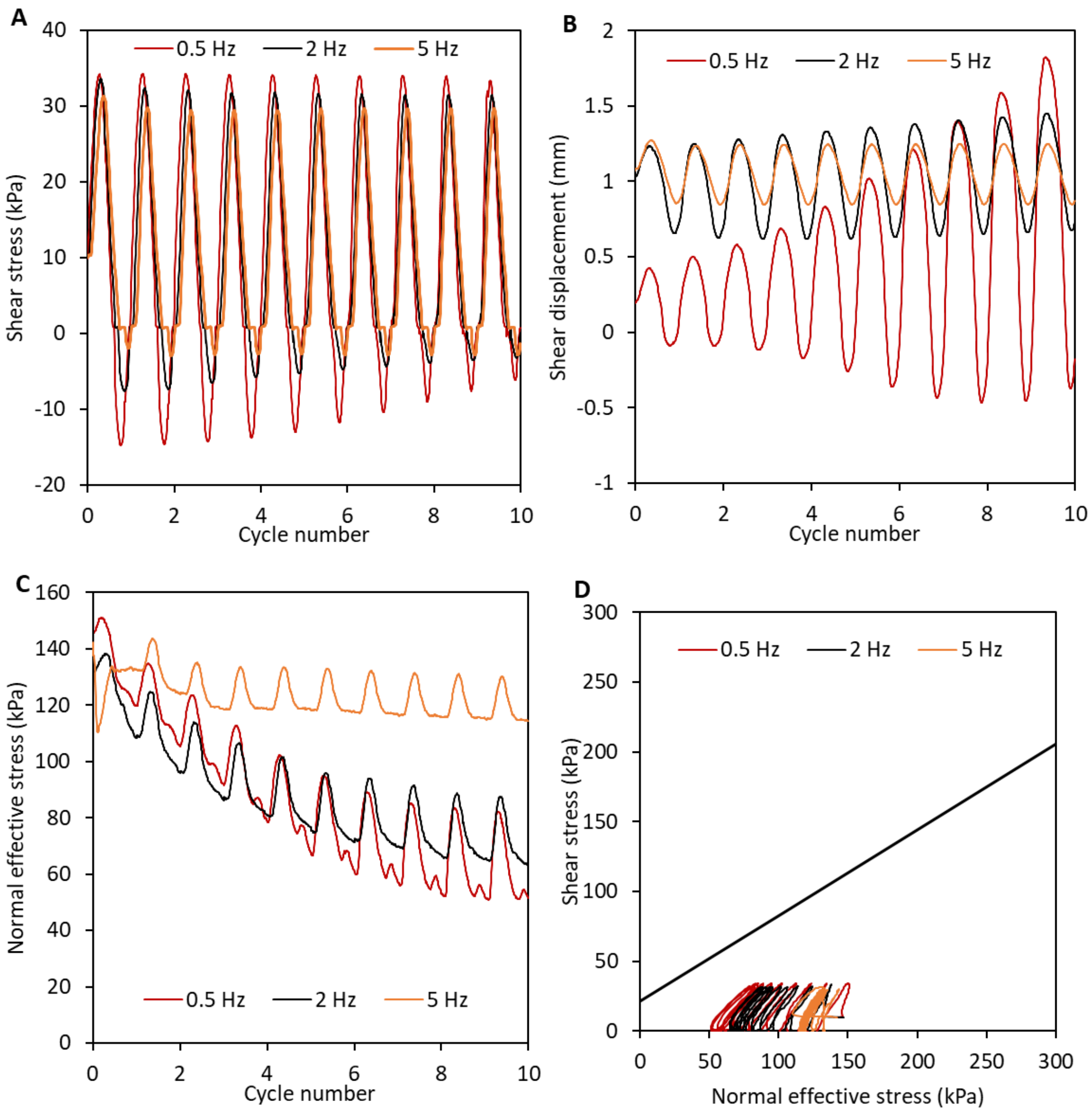

Figure 7. Short duration dynamic shear experiments (10 cycles) conducted at a shear stress amplitude of 25 KPa and frequencies 0.5 Hz, 2 Hz and 5 Hz on sample EN1410C (A) Applied shear stress (B) Measured shear displacement (C) Normal effective stress (D) Stress path in relation to conventional failure envelope

To evaluate the displacement behaviour of the TLC during periods of longer duration dynamic loading, sample EN1410D was subjected to four dynamic shear stages at a frequency of 0.5 Hz for a duration of 60 seconds (30 cycles). As in experiment EN1410C, the initial normal effective stress and shear stress were applied to the sample between each dynamic shear stage whilst the amplitude of applied shear stress was increased at each stage (Table 2, Fig 8 A). Applying the lowest amplitude of dynamic shear stress (+/- 10 kPa) resulted in no permanent displacement or measurable reduction in mean effective stress during dynamic loading. Thus only minor changes in the stress path were observed during this phase of dynamic loading as the sample remained in a stable state (Fig 8D). During the next dynamic shear phase, however (+/- 25 kPa) (Fig 8A), significant permanent displacement was observed (Fig 8B). During this stage dynamic loading resulted in a rapid reduction in mean effective stress (Fig 8 C) until the failure envelope was reached (σ' = 0 kPa τ = 25 kPa) after approximately 20 cycles (Fig 8D). Once the failure envelope was reached the shear surface mobilised and a slight reduction in shear stress was observed as applied shear stress could no longer be sustained (Fig 8 A). This reduction in shear stress however, did not result in liquefaction as the shear stress remained at the failure envelope (approx. 20 kPa, Fig 8A, 8D). Further dynamic shear stages at higher amplitudes (+/- 50 kPa and 60 kPa) produced the same undrained loading behaviour. In both stages dynamic shear resulted in undrained loading, characterised by a rapid reduction in mean effective stress and rapid displacement of the sample once the failure envelope was reached. Although the increase in dynamic shear stresses generated larger shear displacement as the failure envelope was reached, only a moderate reduction in shear stress was observed (Fig 8 B, D) which indicated that the sample could maintain some shear strength rather than undergoing liquefaction (Fig 8 D).

The results demonstrate that, whilst the the excess pore water pressures generated during the longer duration dynamic shear experiment were sufficient to reach the failure envelope, they did not result in liquefaction or runaway failure at any of the loading scenarios tested. Instead, the experiments showed that the shear surface mobilised once the normal effective stress redued to the conventional failure envelope. Shear displacement terminated at the end of dynamic shearing and remobilised by the same mechanism during subsequent dynamic shear stages once the failure envelope was reached. This behaviour was consistent with a conventional frictional sliding model (e.g. refs).

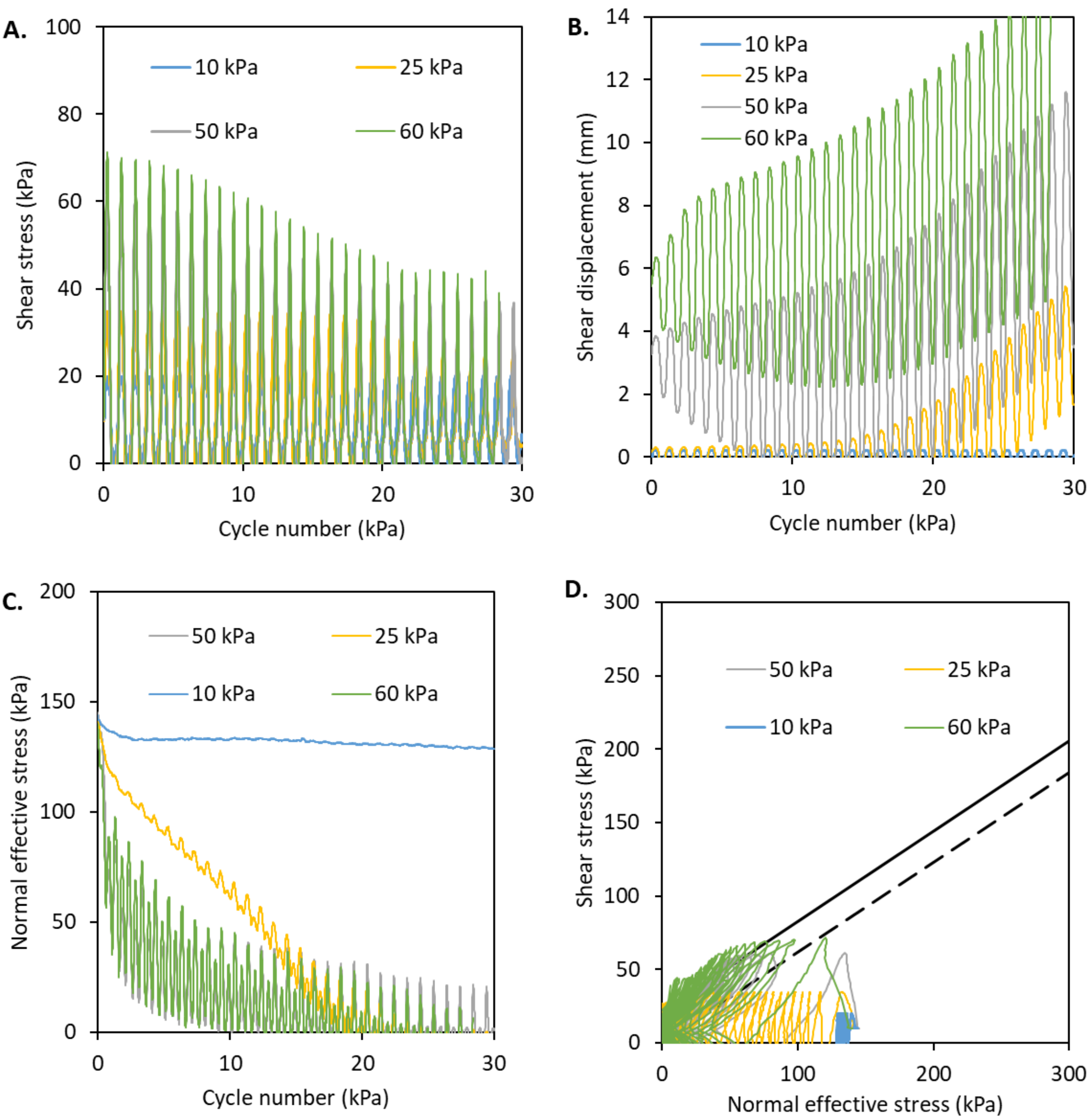

Figure 8. Long duration dynamic shear experiments (30 cycles) conducted at a s frequency of 0.5 Hz at different applied dynamic stress amplitudes on sample EN1410D (A) Applied shear stresses (B) Measured shear displacement (C) Normal effective stress (D) stress path in relation to conventional failure envelope

6. DISCUSSION

A range mechanisms have been proposed to explain subaqueous mass-movement shear surface nucleation (e.g. Viesca and Rice, 2012); shear zone liquefaction and ductile extrusion (e.g. Bull et al., 2009; Sassa et al., 2012); local lateral fluid flow (Dugan and Flemings, 2000; Fleming et al., 2002), and the development of high pore fluid pressures (and thus low effective stress states) by free gas (Carey et al., 2019). Few mechanisms, however, have been proposed to explain the presence of arrested deep-seated submarine landslide complexes subject to large earthquakes. In this study we have undertaken a suite of dynamic shear experiments to explore the potential movement mechanisms in large submarine complexes subject to regular seismic loading events of vary magnitude and duration.

Initial experiments demonstrated that whilst the fine-grained sandy sediments at the base of the Tuehani landslide can liquefy under certain stress conditions at simulated stress states that represent the deeper (40 mbsb), shallow angled (approx. 2°) basal shear zone in the landslide, liquefaction did not occur. Instead permanent displacement is observed when the conventional failure envelope is exceeded by either the increase dynamic shear stress or the decrease in mean effective stress associated with the development of excess porewater pressures.

During both long and short duration dynamic experiments where shear stresses remained low the sediments were unable generate significant pore water pressures. As. As a consequence, effective stress remained high and no measurable displacement occurred. This behaviour is consistent with the lack of evidence of local tsunamigenic waves from landslide movement during the 2016 Kaioura earthquake (Table) and suggested that low amplitude ground shaking from distant earthquakes is unlikely to result in permanent down-slope displacement.

Whilst excess pore water pressurised were generated during short duration dynamic shear experiments conducted at higher shear stress they were not sufficient to reduce the effective stress below the monotonic failure envelope. As a consequence, significant shear displacement did not occur. This suggested that earthquakes producing moderate duration moderate amplitude ground shaking such as the Te Araroa earthquake and earthquakes resulting in short duration high magnitude ground shaking such as Gisborn earthquake are also unlikely to result in landslide movement. In both instances no tsunamigenic waves were recorded consistent with this finding.

During long duration dynamic experiments where shear stress were high permanent displacement did occur. During these experiments dynamic loading of the sediments generated very high pore water pressures that do not result in shear zone liquefaction. Instead critical state behaviour is observed in which shear sliding is initiated once the monotonic failure envelope is reached and is subsequently sustained while normal effective stress remains at or below the monotonic failure envelope. This behaviour suggests landslide movement cam initiate during earthquakes that can generate long duration high amplitude ground shaking such as M8 subduction zone earthquakes. During such events, once mobilised movement would be sustained while mean effective stress remain low and would terminate when the ground shaking is no longer sufficient to sustain a very low normal effective stress within the landslide shear zone,

This style of behaviour provides a mechanism through which the Tuaheni Landslide Complex which could progressively move and arrest downslope without being subject to catastrophic failure, consistent with its current morphology. Many of the previously proposed subaqueous mass movement mechanisms assume that the landslide shear zone requires overpressures which, to date have not been measured the landslide. The sandy nature of the materials allows the development of high excess pore water pressures during seismic loading. High excess porewater pressures within the landslide, however, could reduce the interseismic effective stress conditions in the landslide mass and increase its sensitivity to movement arrest during seismic events.

TABLE 3. SUMMARY OF EARTHQUAKE INDUCE LANDSLIDE TRIGGERING RESULTS

Earthquake description	Catalogued and expected Earthquakes recorded in Gisborne	Local Tsunami recorded	Laboratory simulation
Long duration low amplitude ground shaking associated with distant high magnitude earthquakes	M7.8 Kaikoura earthquake, 2016	No	No significant displacement measured
Moderate duration moderate amplitude ground shaking from high magnitude regional earthquakes	M7.1 Te Araroa earthquake, 2016	No	No significant displacement triggered
Short duration high amplitude ground shaking in response to local shallow crustal earthquakes	M 6.7 Gisborne 2004	No	No significant displacement
Long duration high amplitude shaking in response to local subduction earthquakes	MW 8+ Subduction zone earthquakes (simulated)	No events recorded	Significant displacement triggered

6. CONCLUSIONS

We conducted laboratory experiments in a dynamic back-pressured shearbox on sediments recovered from the base of Tuaheni Landslide Complex to explore styles of movement under conditions that accurately replicate seismic loading. At simulated stress states that represent the deeper (40 mbsb), shallow angled (approx. 2°) basal shear zone in the landslide, liquefaction does not occur. Instead permanent displacement is observed when the conventional failure envelope is exceeded by either the increase dynamic shear stress or the decrease in mean effective stress associated with the development of excess porewater pressures, which result in of balance forces within the system. The amount and rate of displacement is therefore a function of the magnitude and duration of the out of balance forces.

7. ACKNOWLEDGEMENTS

REFERENCES

Allison, R., and Brunsden, D., 1990, Some mudslide movement patterns: Earth Surface Processes and Landforms, v. 15, p. 297-311.

Brain, M.J., Rosser, N.J., Sutton, J., Snelling, K., Tunstall, N., and Petley, D.N., 2015, The effects of normal and shear stress wave phasing on coseismic landslide displacement: Journal of Geophysical Research: Earth Surface, v 120, p. 1009-1022.

Dugan, B., and Flemings. P.B., 2000, Overpressure and fluid flow in the New Jersey continental slope: Implications for slope failure and cold seeps: Science, v. 289, p. 288–291.

Hampton, M. A., Lee, H. J., and Locat, J., 1996, Submarine Landslides: Reviews of Geophysics, v. 34, p. 33-59.

Iverson, R.M., 2005. Regulation of landslide motion by dilatancy and pore pressure feedback: Journal of Geophysical Research, v. 110, F02015.

Kilburn, C.J., and Petley, D.N., 2003. Forecasting giant, catastrophic slope collapse: lessons from Vajont Northern Italy: Geomorphology, v. 54, p. 21-32.

Kossel, E., Bigalke, N., Piñero, E., and Haeckel, M., 2013, The SUGAR Toolbox - A library of numerical algorithms and data for modelling of gas hydrate systems and marine environments, Bremerhaven, PANGAEA .

Mansour, F.M., Morgenstern, N.R., and Martin, D.C., 2011, Expected damage from displacement of slow-moving slides: Landslides, v. 8, p. 117-131.

Masson, D.G., Harbitz, C.B., Wynn, R.B., Pedersen, G., and Lovholt, F., 2006, Submarine landslides: processes, triggers and hazard prediction: Philosophical Transactions of the Royal Society A, v. 364, p. 2009-2039.

Micallef, A., Masson, D.G., Berndt, C., and Stow, D.A.V., 2007, Morphology and mechanics of submarine spreading: A case study from the Storegga Slide: Journal of Geophysical Research, v. 112, F03023.

Mountjoy, J.J., Pecher, I., Henrys, S., Crutchley, G., Barnes, P.M., and Plaza-Faverola, A., 2014, Shallow methane hydrate system controls ongoing, downslope sediment transport in a low-velocity active submarine landslide complex, Hikurangi margin, New Zealand: Geochemistry, Geophysics, Geosystems, v. 15, p. 4137-4156.

Mountjoy, J.J., McKean, J., Barnes, P.M., and Pettinga J.R., 2009, Terrestrial-style slow-moving earthflow kinematics in a submarine landslide complex: Marine Geology, v. 267, p.114-127.

Ng, K-Y., and Petley, D.N., 2009, A process approach towards landslide risk management in Hong Kong: Quarterly Journal of Engineering Geology and Hydrogeology, v. 42, p. 487-498.

Owen, M., Day, S., and Maslin, M., 2007, Late Pleistocene submarine mass movements: occurrence and causes: Quaternary Science Reviews, v. 26, p. 958-978.

Petley, D.N., Higuchi, T., Petley, D.J., Bulmer, M.H. and Carey. J., 2005, The development of progressive landslide failure in cohesive materials: Geology, v. 33, p. 201-204.

Saffer, D.M., and Tobin. H.J., 2011, Hydrogeology and mechanics of subduction zone forearcs: Fluid flow and pore pressure: Annual Review of Earth and Planetary Sciences, v. 39, p. 157-186.

Sassa, K., He, B., Miyagi, T., Strasser, M., Konagai, K., Ostric, M., Setiawan, H., Takara, K., Nagai, O., Yamashiki, and Y., Tutumi, S., 2012, A hypothesis of the Senoumi submarine megaslide in Surga Bay in Japan – based on the undrained dynamic loading ring shear tests and computer simulation: Landslides, v. 9, p. 439-455.

Stigall, J., and Dugan, B., 2010, Overpressure and earthquake initiated slope failure in the Ursa region, northern Gulf of Mexico: Journal of Geophysical Research, v.115, B04101.

Twichell, D. C., Chaytor, J. D., ten Brink, U. S., and Buczkowski, B., 2009, Morphology of late Quaternary submarine landslides along the U.S. Atlantic continental margin: Marine Geology, v. 264, p. 4-16.

Viesca, R. C., and Rice, J.R., 2012, Nucleation of slip-weakening rupture instability in landslides by localized increase of pore pressure: Journal of Geophysical Research, v. 117, B03104.

FIGURE CAPTIONS

.

TABLE CAPTIONS